

Summer 2012 Coop Report

Scott Smale

August 15, 2012

1 Introduction

During the past summer I have had the privilege of working on the TRINAT (TRIumf Neutral Atom Trap) experiment at TRIUMF. The current goal of TRINAT is to measure the beta asymmetry in Potassium 37 as a precision test of the parity violation of the weak force.

Beta decay is a three body decay wherein a nucleon, either a proton or neutron, emits an (anti-)electron and a neutrino and converts into the opposite nucleon. Formally:

$$n \rightarrow p + e^- + \bar{\nu}_e \quad (1)$$

$$\text{or} \quad (2)$$

$$p \rightarrow n + e^+ + \nu_e \quad (3)$$

Note that the proton only decays because the binding energy of the daughter nucleus is larger than the parent nucleus; an isolated proton is stable. In this context electrons are known as beta minus, β^- , particles and positrons are known as beta plus, β^+ , particles. For the purposes of this report it will be sufficient to ignore their charge and to simply refer to these particles as beta particles.

In beta decay the maximally parity violating nature of the weak force manifests itself as an asymmetry in the angular distribution of the decay product beta relative to the nuclear spin of the parent nucleus. This is because the direction of beta emission is correlated to the direction of the neutrino which itself is controlled by the orientation of the neutrino spin relative to the nuclear spin since as far as we know the neutrino is left-handed.

In order to measure beta asymmetry accurately one needs a small cold cloud of atoms with their nuclear spins all aligned along one particular quantization axis, figure 1. The accuracy of the measurement depends on how many nuclei have their spins aligned in the same direction along the quantization axis since if the nuclear spins were arranged randomly there would be no observable asymmetry.

The nucleus can be spin polarized by using the hyperfine coupling between the electron's total angular momentum and the nuclear spin. Photons carry either +1 or -1 angular momentum in units of \hbar . Photons with +1 angular momentum are called σ^+ and those with -1 are called σ^- with both having the interpretation of being circularly polarized with opposite handedness. Photons with +1 angular momentum travelling along the quantization axis will have a chance to be absorbed by the valence electron of a nuclei. The total electron angular momentum quantum number, m_J , will increase by 1. The electron can then emit a photon in any direction and decay back down where it can absorb another and repeat the process. For non-zero nuclear spin, I , the eigenstates of the atom are combinations of states with different m_J and m_I . Thus when a photon is absorbed the state of the system becomes a superposition of states with higher m_J than before and those states also have higher m_I than before. When the electron decays there is no preference for higher or lower m_J so on average there is no change. Thus after repeated absorptions and decays the electron and nucleus are both spin polarized with maximal values of m_J and m_I .

In an ideal world where the laser beam used for spin polarizing was composed of purely σ^+ photons, and there were no other effects, the proportion of nuclei that are spin polarized would be 1. However if the laser beam contains σ^- photons then the degree of polarization of the nuclei will be decreased. This is because the σ^- photons would, on average, be polarizing the nuclei in the opposite direction along the quantization axis. In fact it doesn't matter what direction along the quantization axis the nuclear spins are pointing, only that they are all pointing in the same direction. The important point is that the more pure the beam of

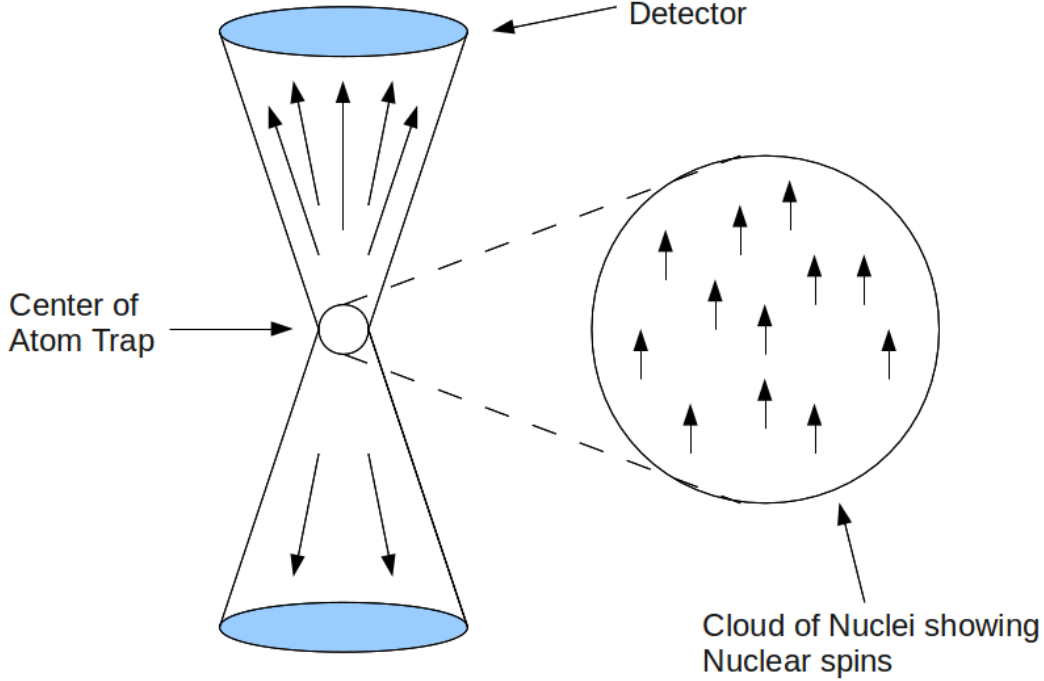


Figure 1: Simple diagram of beta asymmetry showing the asymmetry between the number of betas emitted upwards and the number emitted downwards. Also shown are the nuclear spins with perfect spin polarization.

photons, the better the spin polarization of the nuclei, and the more accurate the measurement that can be made.

2 Testing Circularly Polarized Light

Getting pure circularly polarized light of one handedness to the atom cloud in the center of the trapping chamber is non-trivial due to the detectors. The best position for the detectors is on each end of the quantization axis since then the asymmetry in the number of betas will be maximal. Unfortunately the laser needs to pass through the atom cloud along the quantization axis since the direction of the laser is what defines the quantization axis. The solution is to use mirrors as shown in figure 2. The mirrors are made from a thin silicon carbide, SiC, substrate coated with a multi-layer reflection coating on both sides to prevent the mirrors warping like a potato chip. The substrate is SiC because silicon and carbon are both low Z materials and so will minimize scattering as the beta particles pass through the mirrors. SiC also has a much higher Young's modulus than other low Z candidates for mirror substrates which further reduces the potato chip effect.

My largest task this summer has been to create purely circularly polarized light, either σ^+ or σ^- , and test how well the SiC mirrors preserve the degree of circular polarization after reflection. We cannot measure whether individual photons are σ^+ or σ^- ; we can only average over the beam. To be quantitative about the degree of circular polarization we choose to use a subset of the Stokes parameters. We define:

$$S_{lin} = \frac{P_{max} - P_{min}}{P_{max} + P_{min}} \quad , \quad S_3 = \sqrt{1 - S_{lin}^2} \quad (4)$$

where P_{max} and P_{min} are the maximum and minimum powers obtained when a power meter is placed directly behind a linear polarizer that is rotated around the beam axis a full revolution. For perfectly linearly polarized light the value of S_{lin} will be 1 and the value of S_3 will be 0. Conversely for perfectly circularly polarized light the values of S_{lin} and S_3 will be 0 and 1 respectively. The importance of S_3 is that in theory the proportion of nuclei that are spin polarized will be equal to the average of S_3 and 1.

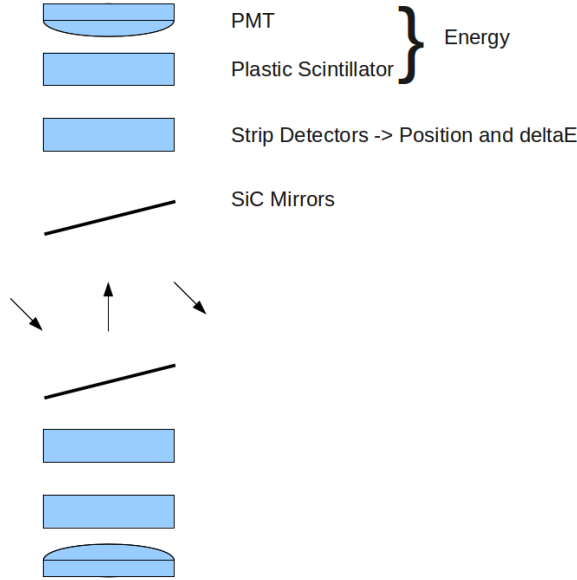


Figure 2: Schematic of the vertical axis of the test chamber. The detectors are along the vertical axis so the laser must enter the chamber at an angle and be reflected between two mirrors. The angle of incidence on each mirror is 9.5° .

I have tried two different configurations for creating circularly polarized light. The first is composed of a fused silica polarizing beam splitter cube as the initial linear polarizer and a polymer quarter waveplate at 45° to the polarizer. The second is composed of a colorPol® polarizer as the initial polarizer and a liquid crystal variable retarder (LCVR) to create the circularly polarized light. The LCVR has its fast and slow axes fixed and an applied voltage changes the amount of retardation between them. The method of measuring S_3 consisted of placing an analyzer polarizer (of the same type as the one used to create the circularly polarized light) in front of a power meter and rotating it to determine the maximum and minimum powers that reach the power meter. These are the P_{max} and P_{min} in equation 4.

Our goal was to achieve S_3 of 0.9997 after one reflection from the mirror at an angle of incidence of 9.5° . The values of S_3 measured as the mirror was rotated through many angles of incidence are shown in figures 3 and 4. Figure 3 shows the results when the silica beamsplitter and quarter waveplate were used. Figure 4 shows the results when the colorPol® polarizer and LCVR were used. The silica beamsplitter and quarter waveplate do not provide a high enough degree of circularly polarized light to meet our criterion. The colorPol® and LCVR combination exceed our expectations by providing $S_3 = 0.999958$ at 9.5° . The slope of the log-log plot for the colorPol® and LCVR data is 5.006. We don't know the physics behind this at the moment but it is something to look at in the future.

3 Fiber Coupling

Ordinarily to get laser light into the chamber from the laser requires a long series of mirrors and other elements. Instead of using many mirrors this time we will be using a fiber optic cable to carry the laser light from the optics table to the top of the test chamber.

The simplest optical fiber is the step index fiber. It is composed of a cylindrical core of a material with a high index of refraction surrounded by a cylindrical shell of low index of refraction material as shown in figure 5. Using ray tracing and Snell's law, any rays with a shallow enough angle entering the end of the fiber will undergo total internal reflection and propagate through the fiber. This angle defines the numerical aperture of the fiber. From a wave perspective a radial cut through the fiber looks like a step potential well. The equations describing the electric field are analogous to Schrodinger's equation in quantum mechanics[1]

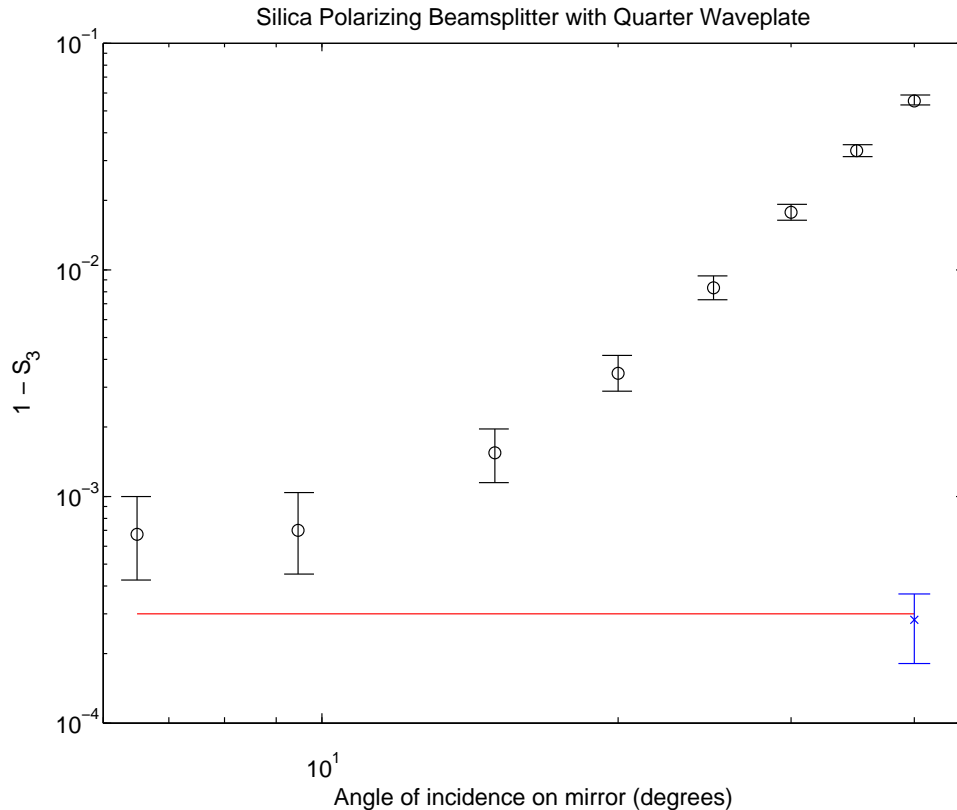


Figure 3: Plot of the difference between 1 and S_3 versus the angle of incidence on the mirror for the silica beamsplitter and quarterwave plate configuration. The cross on the right is the value of S_3 of the light incident on the mirror. The red line represents the goal of $S_3=0.9997$.

and the solutions are the familiar standing waves in the center of the well with exponential decay at each end. In general when light enters this fiber each of the modes has a chance to be excited and carry energy at different speeds through the fiber.

We are using an endlessly single mode fiber which means that over a wide range of wavelengths only one mode can propagate through the fiber. It is more complex than a step index fiber but the same principle of having individual modes that can propagate applies. In particular the mode shape for this fiber should be gaussian. The shape of the mode is important because to achieve the maximum amount of power through the fiber the mode shape of the laser should be identical to that of the fiber. If it is not then the laser will try to excite modes in the fiber that, by virtue of being a single mode fiber, are intentionally absorbed by the fiber. This limits the efficiency of the power transmission through the fiber.

While we cannot at the moment modify the details of the mode shape of the laser we can of course change the overall size of the mode shape by changing the size of the laser beam. It is also necessary to focus the laser beam at the tip of the fiber in all three directions. The focused spot that enters the fiber obviously needs to be centered in the transverse directions but it also needs to be focused to the right location along the beam axis in order to both match the mode size and have a small enough numerical aperture to enter the fiber. To accomplish this we use the setup shown in figure 6. The beam reflects off of two mirrors and into a telescope. The mirrors control the x-y position and the angle of the beam. The telescope allows us to control the beam size by choosing the correct lens combination. After the telescope is a fiber coupling unit sold by Thorlabs with a lens that in theory takes collimated laser light and focuses it onto the fiber tip. The

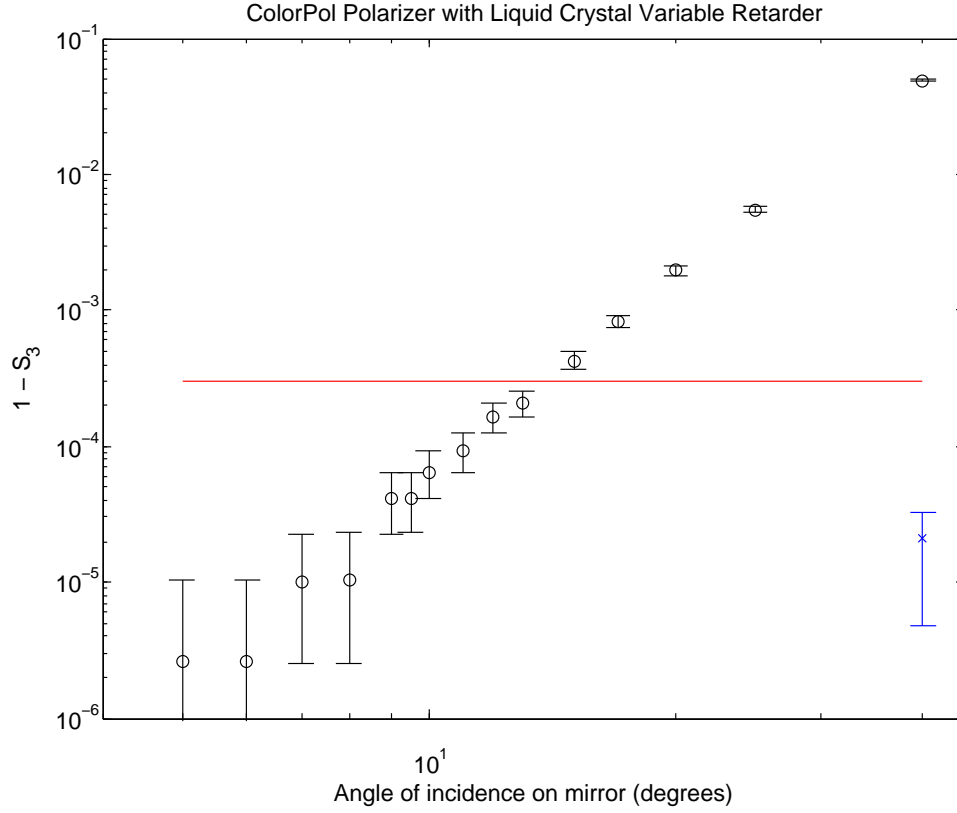


Figure 4: Plot of the difference between 1 and S_3 versus the angle of incidence on the mirror for the colorPol® polarizer and LCVR configuration. The cross on the right is the value of S_3 of the light incident on the mirror. The red line represents the goal of $S_3=0.9997$.

first lens in the telescope is on a z-stage which allows it to control the focus at the fiber tip. Using ray optics and approximations one can show that the relationship between the change in distance of the z-stage, ϵ , is related to the change in distance of the focus at the fiber tip, δ by

$$\delta = \epsilon \left(\frac{f_3}{f_2} \right)^2 \quad (5)$$

where f_2 and f_3 are the focal lengths of the second lens of the telescope and the lens of the Thorlabs unit respectively. So given that $f_3 = 15$ mm and $f_2 \approx 50$ mm the micrometer scale on the z-stage was able to move the focus at the fiber tip by a tenth of a micrometer resolution which is within the expected acceptable tolerance for the focus.

The maximum power efficiency achieved was 57%. While fiber coupling is never perfect, one reason why we have only achieved this efficiency might be due to the details of the mode shape of our laser beam. The beam travels through an acoustic optical modulator (AOM) that alters its frequency. It is unknown what an AOM does to the mode shape of a laser beam so it could be making the mode shape non-gaussian so there would be a mode mismatch with the fiber.

As a diagnostic check we scanned through the travel range of the z-stage holding the first lens while measuring the power through the fiber in an effort to characterize what was happening. One such scan is shown in figure 7. The shape and size of the maxima has many contributing factors but the predominant factor should be the fact that the beam spot is focusing to a finite gaussian focus as shown in figure 8.

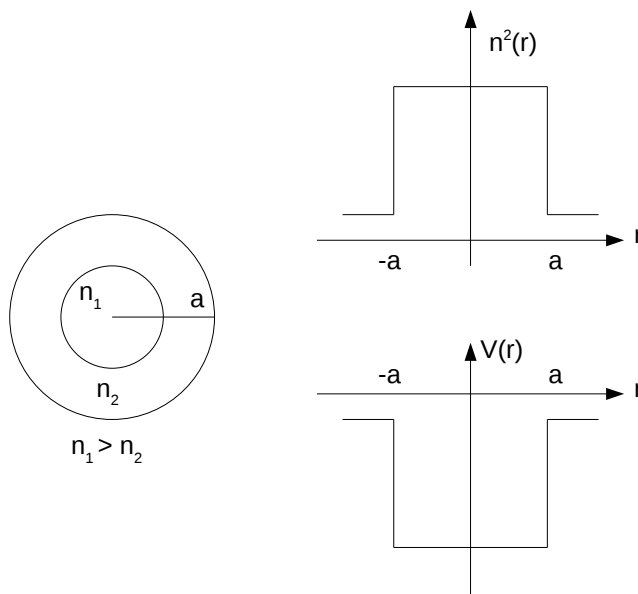


Figure 5: Diagram of step index fiber and the corresponding potential well for the light waves.

Moving the focus along the z -axis corresponds to increasing or decreasing the size of the beam. The maxima should correspond to the z -axis position where the modes of the laser and fiber are matched. The width of the maxima should correspond to the Rayleigh range of the focus, z_R , in figure 8. We find that the expected Rayleigh range and the width of the maxima from scanning the z -stage agree to within an order of magnitude which is acceptable considering the argument above is only approximate. Especially since for some conditions there are actually two maxima in a single scan. The double maxima might be a result of steering as the first lens is moved along the z -axis.

4 Conclusions

The SiC mirrors have been proven to preserve the degree of circularly polarized light better than we expected. The fiber coupling into the endlessly single mode fiber is not as good as hoped but given that 75% efficiency is considered good we feel that it should be acceptable. I have enjoyed my time here and I look forward to the next four months.

References

- [1] Ariel Lipson, Stephen G. Lipson, Henry Lipson, *Optical Physics 4th Edition*. Cambridge University Press, New York.

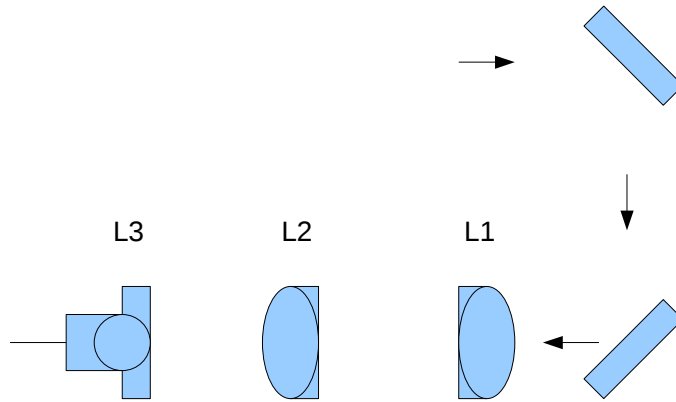


Figure 6: Schematic of the setup used to couple laser light into the optical fiber. The telescope is composed of lenses L1 and L2. Lens L1 is mounted in a z-stage which allows it to move along the beam axis. Both L1 and L2 are mounted such that their lenses can be swapped for ones with different focal lengths and thereby change the magnification of the telescope.

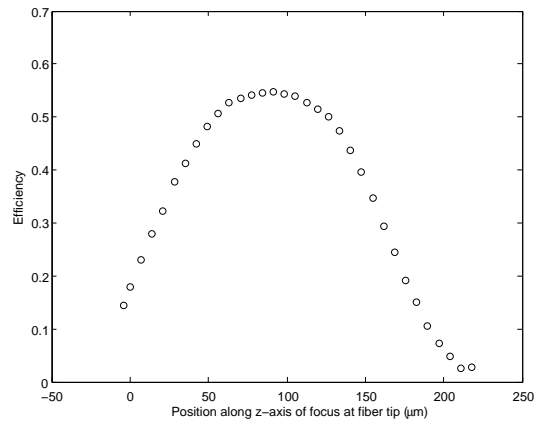


Figure 7: Efficiency versus position of the focus at the fiber tip along the z direction. This is an example of a scan with one maximum.

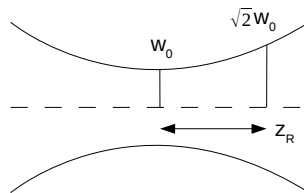


Figure 8: Diagram of step index fiber and the corresponding potential well for the light waves.